# Sarcospan reduces dystrophic pathology: stabilization of the utrophin–glycoprotein complex

Angela K. Peter,[1] Jamie L. Marshall,[1] and Rachelle H. Crosbie[1,2]

[1]Department of Physiological Science and [2]Molecular Biology Institute, University of California, Los Angeles, Los Angeles, CA 90095

Mutations in the dystrophin gene cause Duchenne muscular dystrophy and result in the loss of dystrophin and the entire dystrophin–glycoprotein complex (DGC) from the sarcolemma. We show that sarcospan (SSPN), a unique tetraspanin-like component of the DGC, ameliorates muscular dystrophy in dystrophin-deficient *mdx* mice. SSPN stabilizes the sarcolemma by increasing levels of the utrophin–glycoprotein complex (UGC) at the extrasynaptic membrane to compensate for the loss of dystrophin. Utrophin is normally restricted to the neuromuscular junction, where it replaces dystrophin to form a functionally analogous complex. SSPN directly interacts with the UGC and functions to stabilize utrophin protein without increasing utrophin transcription. These findings reveal the importance of protein stability in the prevention of muscular dystrophy and may impact the future design of therapeutics for muscular dystrophies.

## Introduction

The dystrophin–glycoprotein complex (DGC) is composed of integral and peripheral membrane proteins that span the plasma membrane and connect the extracellular matrix with the intracellular actin cytoskeleton (Campbell and Kahl, 1989; Ervasti et al., 1990, 1991; Yoshida and Ozawa, 1990; Ervasti and Campbell, 1991, 1993). In skeletal muscle, the DGC provides mechanical stability to the sarcolemma during contraction (Petrof et al., 1993). Mutations in the dystrophin gene are responsible for X-linked Duchenne muscular dystrophy (DMD), which is characterized by progressive wasting of skeletal muscles eventually resulting in cardiac and respiratory failure (for review see Durbeej and Campbell, 2002). In DMD patients, loss of dystrophin results in the absence of the entire DGC complex, leading to severe membrane damage and muscle degeneration (for review see Durbeej and Campbell, 2002). *mdx* mice, which are an established model for DMD, possess a genetic mutation in exon 23 of the murine dystrophin gene, resulting in loss of dystrophin protein. As a result, the entire DGC is also absent from the sarcolemma, likely because of rapid protein degradation in the absence of a fully assembled complex. Muscles from *mdx* mice are pathologically similar to DMD patients and display marked membrane disruption as a result of sarcolemmal instability. Akt signaling is hyperactivated in muscles from DMD patients and *mdx* mice (Peter and Crosbie, 2006), suggesting that the DGC may also play a role in cellular signaling in addition to its role in mechanical stability of the sarcolemma (Judge et al., 2006).

The transmembrane proteins of the DGC serve as important anchorages for the peripheral membrane DGC components. These integral membrane proteins include sarcospan (SSPN), the sarcoglycans (SGs; α-, β-, γ-, and δ-SG), and β-dystroglycan (DG; for review see Michele and Campbell, 2003). The SGs and β-DG are single-pass transmembrane glycoproteins. Dystrophin, an actin-binding protein, is localized adjacent to the sarcolemma by attachment to the intracellular N terminus of β-DG (for review see Michele and Campbell, 2003). On the extracellular face of the membrane, β-DG interacts with α-DG to form a receptor for ligands in the extracellular matrix (Ervasti and Campbell, 1993). The SGs form a tight subcomplex with SSPN (Crosbie et al., 1999; Miller et al., 2007). Together, the SG–SSPN subcomplex functions to anchor α-DG attachment to the sarcolemma (Holt and Campbell, 1998). As a whole, the DGC provides a physical linkage across the sarcolemma between the extracellular matrix and the intracellular actin cytoskeleton protecting the membrane from contraction-induced damage (for review see Barresi and Campbell, 2006).

Correspondence to Rachelle H. Crosbie: rcrosbie@physci.ucla.edu

Abbreviations used in this paper: DG, dystroglycan; DGC, dystrophin–glycoprotein complex; DMD, Duchenne muscular dystrophy; GAPDH, glyceraldehyde 3-phosphate dehydrogenase; H&E, hematoxylin and eosin; hSSPN, human SSPN; SG, sarcoglycan; SSPN, sarcospan; Tg, transgene; UGC, utrophin–glycoprotein complex.

The online version of this article contains supplemental material.



The Rockefeller University Press $30.00
J. Cell Biol. Vol. 183 No. 3 419–427
www.jcb.org/cgi/doi/10.1083/jcb.200808027

It is well established that stable interactions among the integral membrane proteins are critical for DGC function and prevention of muscular dystrophy (for review see Durbeej and Campbell, 2002). Despite their importance, the factors that determine the structural integrity of the DGC are not well understood. The observation that SSPN possesses some sequence homology to the tetraspanin superfamily of proteins raises the possibility that SSPN may serve an important role in mediating and stabilizing protein interactions within the DGC (Crosbie et al., 1997, 1998, 1999). The tetraspanins each possess four transmembrane domains and function to cluster and organize transmembrane protein complexes, thereby controlling a wide range of cellular functions (for reviews see Hemler, 2003; Levy and Shoham, 2005). Using a site-directed mutagenesis approach, we have demonstrated that SSPN exhibits the structural characteristics that define the tetraspanin superfamily of proteins (Miller et al., 2007).

As a first test of SSPN function, we generated SSPN transgenic (SSPN transgene [Tg]) mice with moderate (10-fold) levels of SSPN protein overexpression in skeletal muscle (Peter et al., 2007). Forced elevation of SSPN caused a concomitant increase in DGC protein expression but did not disrupt localization of the complex to the sarcolemma. We found that overexpression of exogenous SSPN dramatically reduced endogenous SSPN to levels that were barely detectable, suggesting that SSPN expression is tightly regulated. 10-fold elevation of SSPN disrupted normal interactions within the SG–SSPN subcomplex, which, in turn, weakened α-DG attachment to the sarcolemma (Peter et al., 2007). As a result, assembly of the extracellular matrix was disrupted, giving rise to severe congenital muscular dystrophy in mice with moderate levels of SSPN overexpression (Peter et al., 2007). Furthermore, membrane instability was not detected in 10-fold SSPN-Tg mice, demonstrating that pathogenetic mechanisms resulting from SSPN overexpression are distinct from dystrophin deficiency. Despite our exhaustive efforts, we were never able to isolate free, unassociated SSPN in 10-fold SSPN-Tg muscle, which strongly supports our conclusion that SSPN's toxicity is directly related to its association with other molecules within the sarcolemma.

SSPN-Tg mice with low levels of SSPN overexpression (two- to threefold) were also characterized (Peter et al., 2007). In contrast to SSPN-Tg mice with 10-fold levels of overexpression, SSPN-Tg mice with low levels of SSPN overexpression did not exhibit detectable signs of muscle pathology. DGC levels were mildly up-regulated in these mice, but interactions with the extracellular matrix were not adversely affected. Endogenous SSPN was not affected by this low level of exogenous SSPN expression. Collectively, these findings lead us to conclude that SSPN levels control DGC structure and function. Furthermore, this work leads to the hypothesis that SSPN may function to orchestrate assembly and stability of the DGC.

## Results and discussion

Our previous work has shown that SSPN functions as a tetraspanin to coordinate protein interactions within the DGC (Peter et al., 2007), which led us to rationalize that SSPN expression in dystrophin-deficient muscle might anchor the transmembrane components of the DGC within the sarcolemma. To test this hypothesis, we engineered transgenic mice to overexpress SSPN on the dystrophin-deficient *mdx* background (SSPN-Tg:*mdx*). The *mdx* phenotype is inherited as an X-linked recessive trait, which stems from a premature stop codon in the dystrophin gene, leading to complete absence of the dystrophin protein. The DGC is absent from the sarcolemma of *mdx* muscle likely because of premature degradation of the protein components in the absence of a fully assembled complex (Ohlendieck and Campbell, 1991). For these experiments, we chose to use low (two- to threefold) SSPN-transgenic (SSPN-Tg) mice, lines 31.6 and 29.1, which displayed normal muscle morphology (Peter et al., 2007). SSPN-Tg mice were engineered to carry the human SSPN (hSSPN) gene under control of the human skeletal muscle α-actin promoter, which limited SSPN protein expression to skeletal muscles (Peter et al., 2007). Although human and mouse SSPN proteins are >90% identical at the amino acid level, antibodies specific to human and mouse SSPN permitted us to distinguish between exogenous (human) and endogenous (mouse) SSPN. SSPN-Tg males were crossed with *mdx* females to generate dystrophin-deficient mice carrying the SSPN Tg (SSPN-Tg:*mdx*).

We first investigated whether SSPN overexpression affected membrane association of DGC components in dystrophin-deficient muscle. Indirect immunofluorescence was performed on transverse cryosections of SSPN-Tg:*mdx* quadriceps muscle to determine the subcellular localization of the other DGC components. In addition to the core components of the DGC, we also analyzed the localization of utrophin, a protein closely related to dystrophin. At the postsynaptic region of the neuromuscular junction in wild-type and *mdx* muscle, utrophin replaces dystrophin to form an otherwise identical utrophin–glycoprotein complex (UGC; Matsumura et al., 1992). Analysis of wild-type non-Tg and SSPN-Tg muscle served as positive controls, and *mdx* muscle was used as a negative control. As shown in Fig. 1, DGC expression was robust in positive controls (wild-type non-Tg and SSPN-Tg) but was not detected in negative control samples (*mdx* and SSPN-Tg:*mdx*). As expected, staining for exogenous SSPN (hSSPN) was only detected in SSPN-Tg muscle, and utrophin expression was restricted to the neuromuscular junction in wild-type non-Tg and SSPN-Tg muscles (Fig. 1). In agreement with previous results (Matsumura et al., 1992), we found that utrophin expression was slightly up-regulated in *mdx* muscle at the extrasynaptic sarcolemma. Surprisingly, we found that overexpression of SSPN in *mdx* muscle broadened the localization of utrophin protein so that it was no longer restricted to the neuromuscular junction but was present throughout the sarcolemma (Fig. 1). Grady et al. (2000) have demonstrated that expression and localization of the UGC is important for proper synaptic formation and clustering of acetylcholine receptors at the postsynaptic membrane. Introduction of utrophin in dystrophin-deficient muscle broadens localization of the UGC to the extrasynaptic sarcolemma, where it ameliorates muscular dystrophy (Tinsley et al., 1996, 1998). The observation that utrophin is localized to the extrasynaptic sarcolemma in SSPN-Tg:*mdx* muscle raises the possibility that utrophin displays elevated protein levels leading to the observed increased

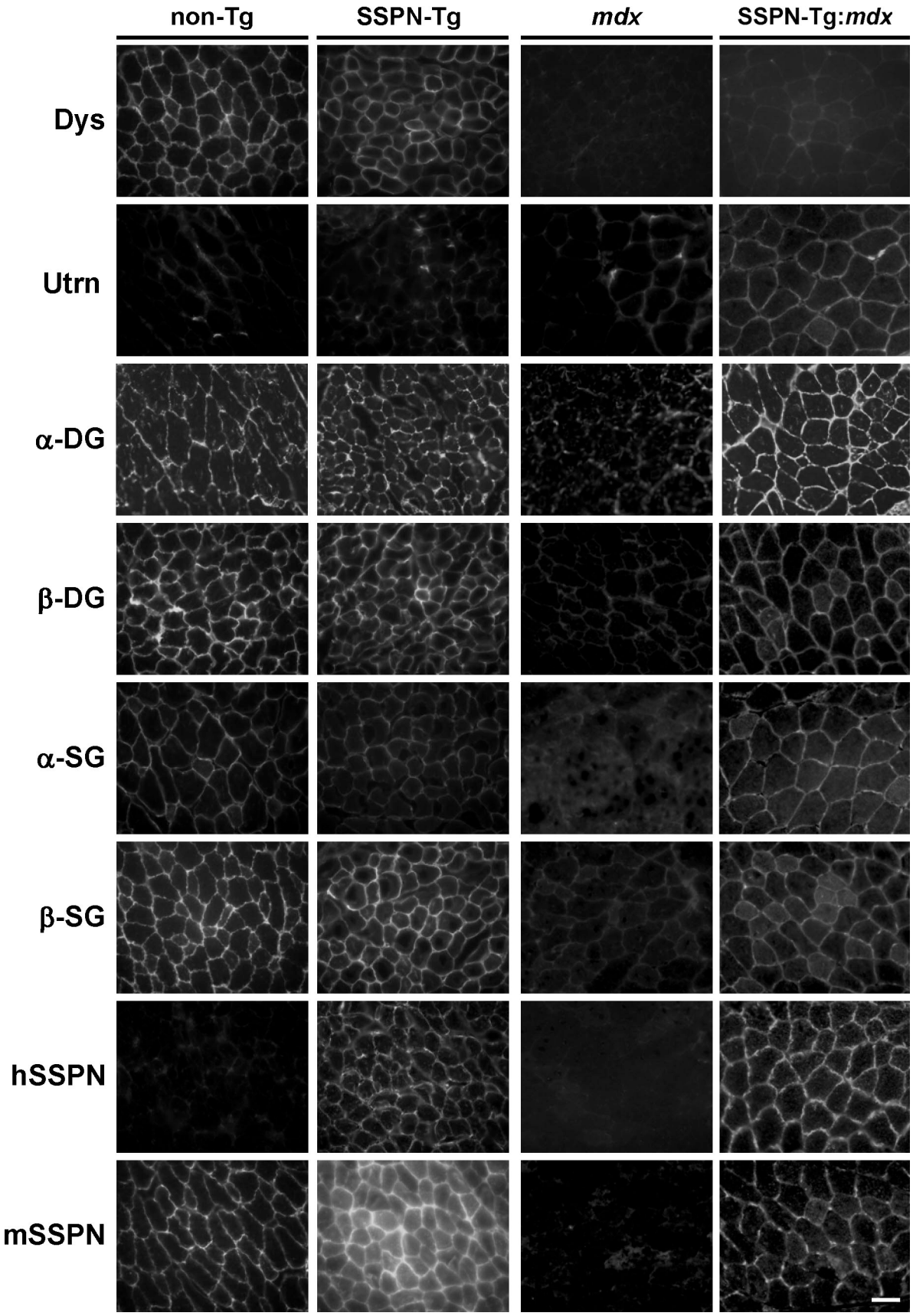


Figure 1. **SSPN stabilizes the UGC at the sarcolemma.** Transverse cryosections of quadriceps muscle from non-Tg (wild type), SSPN-Tg (wild type), *mdx*, and SSPN-Tg:*mdx* mice were stained with the antibodies to dystrophin (Dys), utrophin (Utrn), DGs (α- and β-DG), mouse SSPN (mSSPN), transgenic hSSPN, and SGs (α- and β-SG). Protein staining was visualized by indirect immunofluorescence. Bar, 100 μm.

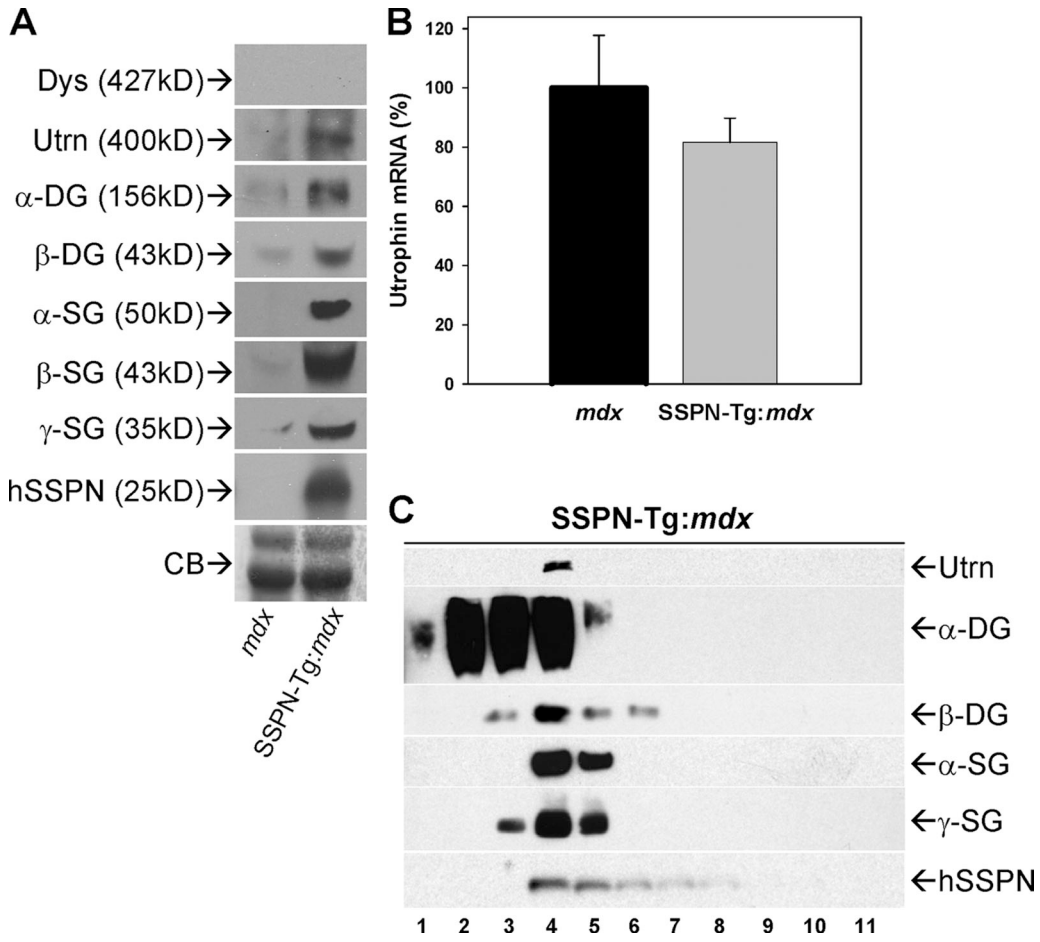


Figure 2. **SSPN regulates UGC levels by interacting directly with this complex.** (A) Skeletal muscle from *mdx* and SSPN-Tg:*mdx* tissue was solubilized in modified radioimmunoprecipitation assay buffer, and 60-µg protein samples were resolved by SDS-PAGE and immunoblotted using antibodies against dystrophin (Dys), utrophin (Utrn), DGs (α- and β-DG), exogenous SSPN (hSSPN), and SGs (α-, β-, and γ-SG). As expected, exogenous hSSPN was only detected in SSPN-Tg:*mdx* muscle. Expression levels of DGs and SGs were dramatically elevated in SSPN-Tg:*mdx* muscle samples. Utrophin, a homologue of dystrophin, is up-regulated in SSPN-Tg:*mdx* tissue. Equal loading of *mdx* and SSPN-Tg:*mdx* lysates was confirmed by Coomassie blue (CB) staining. Molecular masses of individual proteins are indicated in parentheses. (B) Quantitative RT-PCR analysis was used to determine the level of utrophin mRNA in both SSPN-Tg:*mdx* and *mdx* tissue. Data are normalized to GAPDH controls and are represented relative to control values (100%). Utrophin mRNA levels were not statistically different (standard *t* test; P = 0.258) between SSPN-Tg:*mdx* and *mdx* controls, suggesting that SSPN-Tg expression did not affect utrophin transcription. Values represent mean ± SEM (error bars). (C) SSPN is a core component of the UGC in SSPN-Tg:*mdx* mice. Purified UGC proteins were separated by ultracentrifugation through 5–30% sucrose gradients. Fraction 1 represents the lightest region of the gradient. Fractions were analyzed by immunoblotting with antibodies to utrophin (Utrn), DGs (α- and β-DG), SGs (α-, and γ-SG), and exogenous SSPN (hSSPN) as indicated. SSPN and utrophin are enriched in fraction 4, demonstrating that SSPN is a core component of the UGC. The molecular mass of each component is identical to that indicated in A.

sarcolemmal localization and possible functional replacement of the DGC. We also found that SSPN overexpression in *mdx* muscle increased α-/β-DG as well as α-/β-SG levels at the sarcolemma (Fig. 1). These data suggest that SSPN has restored expression of a complete UGC at the sarcolemma in *mdx* muscle, where it may functionally compensate for the loss of dystrophin and its associated proteins.

To determine how SSPN expression affects UGC protein levels, skeletal muscle lysates from 6-wk-old *mdx* and SSPN-Tg:*mdx* mice were analyzed by immunoblotting with antibodies to each of the UGC components. To confirm expression of the Tg, immunoblots were probed with antibodies specific to hSSPN. Exogenous SSPN was abundant in SSPN-Tg:*mdx* muscle samples, demonstrating that stable SSPN protein was produced from the Tg (Fig. 2 A). Levels of α- and β-DG as well as α-, β-, and γ-SG were dramatically increased in SSPN-Tg:*mdx* mice relative to *mdx* controls (Fig. 2 A). DG and SG protein expression in SSPN-Tg:*mdx* muscle was identical to age-matched non-Tg (wild type) muscle (Fig. 2 A and not depicted). As expected, dystrophin protein was not detected in samples from either *mdx* or SSPN-Tg:*mdx* mice. Utrophin protein levels were elevated in SSPN-Tg:*mdx* muscle relative to *mdx* muscle (Fig. 2 A). To investigate whether SSPN increased utrophin expression by enhancing transcription, we performed quantitative RT-PCR analysis. Utrophin mRNA levels were similar in SSPN-Tg:*mdx* and *mdx* muscle (Fig. 2 B). This finding demonstrates that utrophin up-regulation by SSPN does not involve transcriptional regulation. Furthermore, these data suggest that SSPN maintains utrophin protein at the sarcolemma by providing a tetraspanin scaffold, which stabilizes and promotes protein interactions.

We established that SSPN is a core component of the DGC using rigorous biochemical methods (Crosbie et al., 1997, 1998).

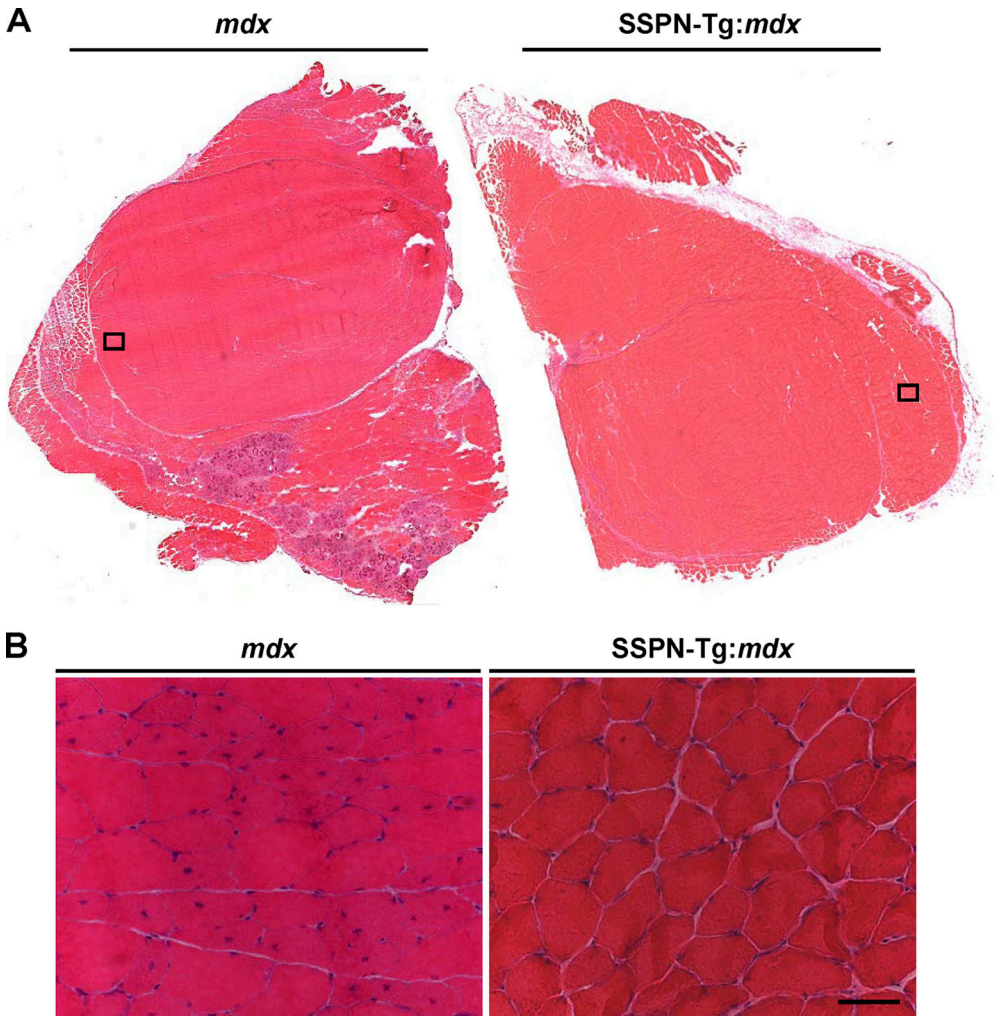


Figure 3. **SSPN-Tg:*mdx* mice display near normal muscle pathology.** (A) Transverse cryosections of whole quadriceps muscle from age-matched *mdx* and SSPN-Tg:*mdx* mice were stained with H&E to visualize muscle pathology. Many necrotic patches are visible in *mdx* quadriceps. Necrotic fibers were never observed in SSPN-Tg:*mdx* quadriceps. Boxed regions indicated on H&E staining of quadriceps muscle from *mdx* and SSPN-Tg:*mdx* mice are shown at higher magnifications in B. Note the presence of numerous myofibers with central nucleation as well as the variation in fiber size evident in *mdx* tissue. Muscle from SSPN-Tg:*mdx* muscle displays reduced central nucleation and improvements in fiber size variation. Bar, 100 μm.

In normal skeletal muscle, SSPN is enriched at the postsynaptic region of the neuromuscular junction in a utrophin-dependent manner (Crosbie et al., 1999). Our findings that SSPN expression alters utrophin localization and, conversely, that SSPN enrichment at the neuromuscular junction is dependent on utrophin suggest that SSPN functions to regulate utrophin through direct association with the UGC. To biochemically determine whether SSPN is a core component of the UGC, we isolated this complex from skeletal muscle of SSPN-Tg:*mdx* mice using lectin affinity chromatography followed by ultracentrifugation on 5–30% sucrose gradients. Only proteins that are tightly associated will be maintained as a complex and migrate together during ultracentrifugation (Crosbie et al., 1997, 1998). Fractions were collected and analyzed by immunoblotting with antibodies to components of the UGC. We found that SSPN protein is highly enriched in fraction 4, which contains utrophin and utrophin-associated proteins (Fig. 2 C). We conclude that SSPN regulates utrophin levels in a mechanism that involves direct association of SSPN with the UGC.

To investigate the functional consequences of increased UGC levels in dystrophin-deficient muscle, we examined SSPN-Tg:*mdx* muscle for dystrophic pathology. *mdx* pathology is characterized by progressive muscle degeneration, compensatory hypertrophy, and necrosis of damaged muscle fibers. Histological analysis was performed by staining transverse cryosections of quadriceps muscle with hematoxylin and eosin (H&E). Images of whole quadriceps muscle taken from *mdx* mice revealed numerous patches of necrosis, which were not present in SSPN-Tg:*mdx* muscle (Fig. 3 A). Central nucleation, a marker of myofiber regeneration, was quantitated by analyzing H&E-stained quadriceps muscle at higher magnification (Fig. 3 B). *mdx* muscles at 6 wk of age display elevated levels (60%) of regenerated myofibers with central nuclei (Fig. 4 A). We found a dramatic (40%) reduction in central nucleation in muscle from SSPN-Tg:*mdx* mice (Fig. 4 A). Although the level of centrally nucleated fibers in SSPN-Tg:*mdx* mice remained slightly elevated compared with non-Tg controls, this is likely explained by fiber to fiber variation in promoter activation (unpublished data).

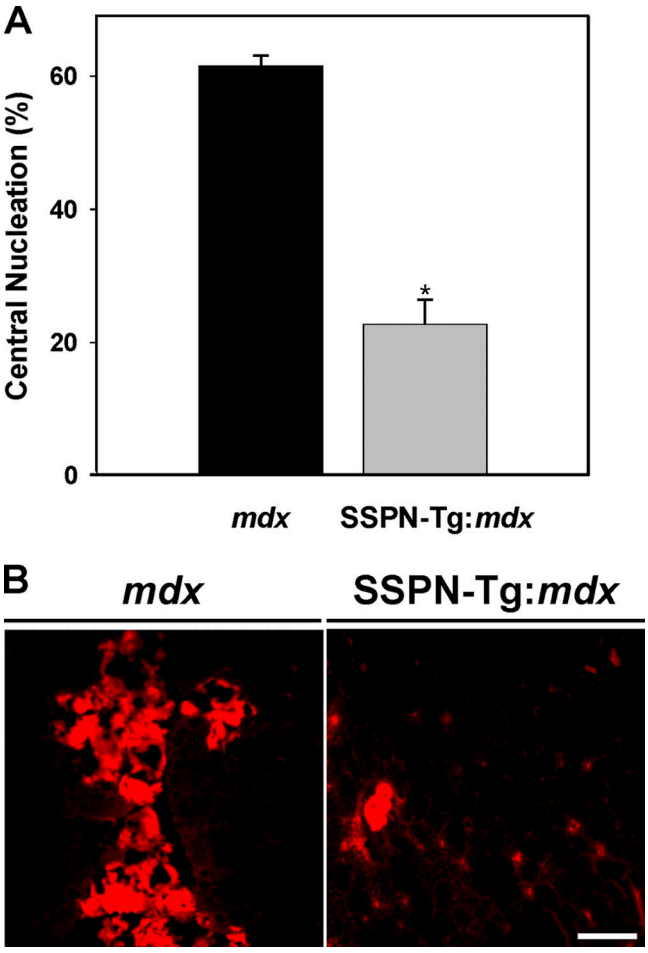


Figure 4. **SSPN improves muscle degeneration and sarcolemmal stability.** (A) Central nucleation (percent of total fibers) was quantified for quadriceps isolated from *mdx* and SSPN-Tg:*mdx* ($n$ = 4). SSPN-Tg:*mdx* mice display a threefold reduction in central nuclei compared with *mdx* age-matched controls. Each value represents mean ± SEM (error bars) of the total quadriceps analyzed (*, $P = 6.0 \times 10^{-4}$). (B) To examine infiltration of blood serum proteins into damaged muscle fibers, *mdx* and SSPN-Tg:*mdx* mice were intraperitoneally injected with Evans blue dye, a marker for membrane instability. *mdx* quadriceps displays many Evans blue dye–positive fibers (visualized by red fluorescence), which is a marker for membrane damage. Evans blue dye was not detected in muscle from SSPN-Tg:*mdx* mice, demonstrating that SSPN expression restored membrane stability in dystrophin-deficient muscle. Bar, 20 µm.

In addition, expression of SSPN in *mdx* mice was associated with a reduction in the number of smaller, atrophic muscle fibers (Fig. S1, available at http://www.jcb.org/cgi/content/full/jcb.200808027/DC1). This reduction of small, newly regenerating fibers provides an additional measure of muscle pathology and is similar to the results reported for microdystrophin (Gregorevic et al., 2006).

Loss of the DGC from the sarcolemma causes membrane instability, which is the primary defect of dystrophin-deficient muscular dystrophy (Weller et al., 1990; Menke and Jockusch, 1991; Petrof et al., 1993; Straub et al., 1997). Unrepaired tears in the sarcolemma allow proteins that are normally restricted to the blood serum to freely diffuse across the sarcolemma and accumulate in the sarcoplasm. To further test the functionality of the UGC in SSPN-Tg:*mdx* mice, we performed a tracer assay with fluorescent Evans blue dye that binds albumin in blood serum (Straub et al., 1997). *mdx* mice displayed severe sarcolemmal fragility marked by Evans blue dye accumulation in numerous muscle fibers (Fig. 4 B). In contrast, we never observed Evans blue–positive fibers in SSPN-Tg:*mdx* tissue (Fig. 4 B).

In this study, we provide biochemical evidence that SSPN ameliorates dystrophic pathology in *mdx* mice by stabilizing the UGC at the sarcolemma through direct interaction with this complex. We demonstrate that SSPN causes redistribution of the UGC to the extrasynaptic sarcolemma, where it functionally replaces the DGC. The primary defect in dystrophin-deficient mice is the loss of sarcolemma integrity, and we demonstrate that SSPN provides stability to the sarcolemma. These data suggest that the actin-UGC–extracellular matrix connection is fully and functionally restored. Future studies will be performed to determine whether SSPN overexpression improves muscle strength in *mdx* mice.

Tinsley et al. (1996, 1998) have shown that increased expression of utrophin in *mdx* mice rescues muscular dystrophy by stabilizing the UGC at the sarcolemma in a dose-dependent manner. Complete reduction of *mdx* pathology to normal wild-type levels (as determined by central nucleation and muscle strength measurements) occurred when utrophin was overexpressed at twice the levels of *mdx* mice (note that endogenous utrophin levels are already up-regulated in *mdx* muscle compared with wild-type controls). Their data nicely show that pathology was directly correlated with the level of utrophin overexpression. Lower levels of utrophin expression reduced the pathology, but not completely back to normal levels. Based on these findings, we speculate that increasing the level of SSPN overexpression would have an even greater impact on improving *mdx* pathology.

Overexpression of DGC proteins, signaling molecules, and compensatory molecules can improve the pathology of muscle fibers in the *mdx* mouse. Utrophin, dystrophin, integrin, neuronal nitric oxide synthase, and cytotoxic T cell *N*-acetylgalactosamine transferase have been shown to improve muscular dystrophy. Most of these efforts have been focused on the use of dystrophin and utrophin to restore normal muscle function in *mdx* mice. Elegant work from Chamberlain's group has established that full-length (DelloRusso et al., 2002) and internally truncated forms of dystrophin are highly effective at ameliorating *mdx* pathology in addition to increasing muscle strength (for review see Odom et al., 2007). SSPN is unique and offers numerous advantages over current therapeutic strategies. The SSPN cDNA is under 1 kb, which is well within the range for easy packaging into adeno-associated viral vectors for delivery, circumventing the necessity to generate recombinant forms of SSPN. Because SSPN is expressed in a variety of nonmuscle tissues, even in dystrophin deficiency, increasing the expression of SSPN in skeletal muscle should not pose an immune threat. One therapeutic angle for the treatment of DMD is to identify small molecules that up-regulate utrophin protein expression. Our findings now establish that SSPN regulates utrophin protein levels and localization within the myofiber.

The results in this study were unexpected because, for nearly 10 yr, the precise function of SSPN has remained elusive. Our experiments show that SSPN is a critical mediator of protein

interactions within UGC and raise the possibility that SSPN contributes to the assembly and targeting of the UGC. This is impressive considering that SSPN, the smallest member of the complex, must orchestrate proper structural arrangement of over seven large peripheral and integral membrane proteins. These properties are unique to SSPN and suggest that gene therapeutic strategies targeting SSPN expression may be beneficial for the treatment of DMD.

## Materials and methods

**Generation of SSPN-Tg:*mdx* mice**

Transgenic constructs were engineered with the human skeletal actin promoter and the VP1 intron upstream of hSSPN as described previously (Crawford et al., 2000; Spencer et al., 2002; Peter et al., 2007). SSPN transgenic males, line 29.1, were bred with *mdx* females (The Jackson Laboratory) to produce male SSPN-Tg:*mdx* mice. Female SSPN-Tg (wild type) and non-Tg (wild type) mice as well as male non-Tg:*mdx* littermates were used as controls. Mice were analyzed at 6 wk of age. Transgenic mice used for this study expressed an approximately twofold increase in SSPN protein expression in skeletal muscle compared with non-Tg (wild type) mice (Peter et al., 2007). All mice were maintained in the Life Sciences Vivarium, and all procedures were carried out in accordance with guidelines set by the University of California, Los Angeles Institutional Animal Care and Use Committee.

**Immunofluorescence**

Quadriceps from female SSPN-Tg (wild type), female non-Tg (wild type), male non-Tg:*mdx*, and SSPN-Tg:*mdx* littermates were dissected from 6-wk-old mice. Muscles were covered in 10.2% polyvinyl alcohol/4.3% polyethylene glycol and rapidly frozen in liquid nitrogen–cooled isopentane. Mounted muscle was stored at −80°C until analyzed. 8-µm transverse sections were prepared using a cryostat (CM 3050S; Leica) and stored on positively charged glass slides (VWR). Sections were stored at −80°C for future analysis. Sections were acclimated to RT for 15 min and blocked using 3% BSA diluted in PBS for 1 h at RT. Sections were then incubated at 4°C for 18 h with antibodies to the following proteins (antibody dilutions are indicated): dystrophin (MANDYS1, 1:10; Developmental Studies Hybridoma Bank), utrophin (NCL-DRP2, 1:5; Vector Laboratories), α-DG (IIH6C-4, 1:100; Upstate Signaling), β-DG (MANDAG2, 1:50; Developmental Studies Hybridoma Bank), α-SG (VP-A105, 1:100; Vector Laboratories), β-SG (VP-B206, 1:50; Vector Laboratories), hSSPN (affinity-purified rabbit 15, 1:25), and mouse SSPN (affinity-purified rabbit 18, 1:25). Polyclonal antibodies to endogenous (mouse) and exogenous (human) SSPN have been described previously (Peter et al., 2007). Primary antibodies were detected by FITC-conjugated anti–rabbit and anti–mouse (Jackson ImmunoResearch Laboratories and Millipore) secondary antibodies diluted at 1:500. Secondary antibodies were incubated for 1 h at RT. To preserve the fluorescence signal, sections were mounted in Vectashield (Vector Laboratories). To determine the level of nonspecific staining, secondary antibodies alone were incubated with sections. Mounted sections were visualized using a fluorescent microscope (Axioplan 2; Carl Zeiss, Inc.) equipped with a Plan Neofluar 40× NA 1.3 oil differential interference contrast objective, and images were captured using Axiovision 3.0 software (Carl Zeiss, Inc.).

**Evans blue tracer assay**

To establish sarcolemmal integrity, mice were injected with 50 µl of Evans blue dye (10 mg/ml in 10 mM of sterile phosphate buffer and 150 mM NaCl, pH 7.4) per 10 g of body weight as described previously (Straub et al., 1997). Peritoneal cavity injection was performed on 6-wk-old SSPN-Tg:*mdx* and non-Tg:*mdx* littermates. 24 h after injection, quadricepses were excised and mounted as described in the Immunofluorescence section. 8-µm transverse sections were briefly fixed in ice-cold acetone, washed in PBS (10 mM phosphate buffer and 150 mM NaCl, pH 7.4), and mounted with Vectashield. Evans blue–positive myofibers were observed using an Axioplan 2 fluorescent microscope and a Plan Neofluar 40× NA 1.3 oil differential interference contrast objective.

**Histology**

H&E staining was used for visualization of fibrosis, central nuclei, and fiber diameter. 8-µm transverse quadriceps sections were left at RT for 15 min before beginning the staining procedure. Sections were incubated with hematoxylin for 3 min, washed with water for 1 min, incubated with eosin for 3 min, and dehydrated in solutions of 70, 80, 90, and 100% ethanol. Sections were then incubated in xylene for a total of 6 min. Sections were left at RT briefly to dry before mounting with Permount. All supplies for the H&E staining were purchased from Thermo Fisher Scientific.

To measure the fiber area and count centrally nucleated fibers, digitized images were captured under identical conditions using an Axioplan 2 fluorescent microscope and Axiovision 3.0 software (Carl Zeiss, Inc.). The percentage of centrally nucleated fibers and fiber areas were assessed for four SSPN-Tg:*mdx* and four non-Tg:*mdx* mice. Data for central nucleation are represented as a percentage of the total fibers counted. Fiber areas and central nucleation percentages were averaged, and the standard error is represented. Sigma Plot software (Systat Software, Inc.) was used to perform statistical analysis. Entire quadriceps images were attained using a microscope (AxioImager M1, Carl Zeiss, Inc.) and Axiovision Rel. 4.5 software (Carl Zeiss, Inc.).

**Protein preparation**

Skeletal muscle was snap frozen in liquid nitrogen and ground to a fine powder with a mortar and pestle. Pulverized muscle was added to ice-cold modified radioimmunoprecipitation assay lysis buffer with phosphatase inhibitors (1% Nonidet P-40, 0.5% sodium deoxycholate, 0.1% SDS, 1 mM EDTA, 5 mM *N*-ethylmaleimide, 50 mM sodium fluoride, 2 mM β-glycerophosphate, 1 mM sodium orthovanadate, 100 nM okadaic acid, 5 nM microcystin-L-arginine, and 20 mM Tris-HCl, pH 7.6) and protease inhibitors (0.6 µg/ml pepstatin A, 0.5 µg/ml aprotinin, 0.5 µg/ml leupeptin, 0.75 mM benzamidine, and 0.1 mM PMSF). Homogenates were rocked at 4°C for 1 h. After clarification by centrifugation at 15,000 *g* for 15 min, tissue lysates were stored at −80°C.

**Immunoblot analysis**

Protein concentrations were determined using the DC Protein Assay (Bio-Rad Laboratories). Equal concentrations (60 µg) of protein samples were resolved by 5, 10, or 15% SDS-PAGE and transferred to nitrocellulose membranes (Millipore) for subsequent immunoblotting. Primary antibodies against dystrophin (MANDYS1, 1:10), utrophin (NCL-DRP2, 1:5), α-DG (IIH6C-4, 1:1,000), β-DG (MANDAG2, 1:250), α-SG (VP-A105, 1:100), β-SG (VP-B206, 1:100), γ-SG (VP-G803, 1:100; Vector Laboratories), and hSSPN (affinity-purified rabbit 15, 1:500) were incubated at RT while shaking for 18 h. Horseradish peroxidase–conjugated anti–rabbit IgG (GE Healthcare) and anti–mouse IgG (GE Healthcare) and IgM (Upstate Signaling) secondary antibodies were used at 1:3,000 dilutions. All immunoblots were developed using enhanced chemiluminescence (SuperSignal West Pico Chemiluminescent Substrate; Thermo Fisher Scientific).

**Purification of the UGC**

0.1 g/ml of SSPN-Tg:*mdx* total skeletal muscle protein samples was prepared using standard DGC solubilization buffer (50 mM Tris-HCl, pH 7.8, 500 mM NaCl, and 1% digitonin) and protease inhibitors (0.6 µg/ml pepstatin A, 0.5 µg/ml aprotinin, 0.5 µg/ml leupeptin, 0.75 mM benzamidine, 0.1 mM PMSF, 5 µM calpain I, and 5 µM calpeptin; Crosbie et al., 1998). Homogenates were rocked at 4°C for 1 h. After clarification by centrifugation at 15,000 *g* for 20 min, lysate was then rotated overnight at 4°C with 1 ml agarose-bound succinylated WGA (AL-1023; Vector Laboratories). Succinylated WGA agarose was washed by rotating samples at 4°C four times for 10 min with wash buffer (50 mM Tris-HCl, pH 7.8, 500 mM NaCl, and 0.1% digitonin), including protease inhibitors (0.75 mM benzamidine, 0.1 mM PMSF, 5 µM calpain I, and 5 µM calpeptin) to remove unbound proteins. Bound proteins were eluted with 0.3 M *N*-acetylglucosamine (Sigma-Aldrich) and concentrated using columns (Centricon Ultracel; Millipore) by centrifugation at 4,000 *g* for 20 min. Protein concentration was determined with the DC Protein Assay. A 200-µg sample was layered on top of a 5–30% sucrose gradient prepared by adding 6 ml of a 5% sucrose solution into an open top centrifuge tube (Polyclear; Seton) using a 14-gauge Hamilton syringe and underlaying with an equal volume of a 30% sucrose solution. Gradients were mixed using the Gradient IP station (Biocomp). Sucrose gradients were centrifuged at 35,000 *g* in an ultracentrifuge (Optima L-90K; Beckman Coulter) for 12 h at 4°C using an SW41 rotor (Beckman Coulter). 12 1-ml fractions were collected, and 80 µl of each fraction was resolved by 8% isocratic or 4–20% gradient SDS-PAGE and transferred to nitrocellulose membranes for subsequent immunoblotting. All immunoblotting was performed as described in the previous section with the exception of utrophin (MANCHO3, 1:200; Developmental Studies Hybridoma Bank), which was incubated at 4°C.

### RNA extraction and quantitative PCR analysis

RNA was extracted from snap-frozen total skeletal muscle from male non-Tg:*mdx* and SSPN-Tg:*mdx* littermates using a RiboPure kit (Ambion) as per the manufacturer's instructions. Purified RNA was quantitated using a spectrophotometer (DU 640; Beckman Coulter) as described in the RiboPure instruction manual. Equal RNA concentrations (2.3 µg) were reverse transcribed using a high-capacity cDNA reverse transcription kit (Applied Biosystems) as described by the manufacturer. Reverse transcription was performed on a Mastercycler Gradient (Eppendorf) using the following conditions: 25°C for 10 min, 37°C for 120 min, 85°C for 5 s, and held at 4°C.

Quantitative PCR analysis was performed using POWER SYBR green PCR master mix (Applied Biosystems). Glyceraldehyde 3-phosphate dehydrogenase (GAPDH) was specifically amplified using GAPDH forward (5′-ACTCCACTCACGGCAAATTC-3′) and GAPDH reverse (5′-TCTCCATGGTGGTGAAGACA-3′) primers, which specifically amplified a 171-bp target sequence in mouse GAPDH cDNA. Utrophin cDNA was amplified using utrophin forward (5′-GGGGAAGATGTGAGAGATTT-3′) and utrophin reverse (5′-GTGTGGTGAGGAGATACGAT-3′) primers as previously described (Jasmin et al., 1995). These primers specifically amplified a 548-bp target of the mouse utrophin sequence. All primers were used at a 10-µM concentration. cDNA was diluted 1:10 in RNase/DNase-free water. 1 µl of diluted cDNA was added to 12 µl of 2× PCR master mix, 11 µl RNase/DNase-free water, and 0.5 µl of forward and reverse primers. Quantitative PCR analysis was performed using a single color real-time PCR detection system (MyiQ iCycler; Bio-Rad Laboratories). An initial denaturation cycle was performed at 94°C for 2 min. A total of 40 cycles consisting of denaturation at 94°C for 30 s, primer annealing at 60°C for 30 s, and extension at 72°C for 30 s were performed. A final extension at 72°C was performed for 10 min. Data analysis was performed using MyiQ Optical System software version 1.0 (Bio-Rad Laboratories). Levels of utrophin mRNA were normalized to GAPDH controls, and SSPN-Tg:*mdx* samples are represented relative to *mdx* controls (100%). Statistical analysis was performed using the standard *t* test.

### Online supplemental material

Fig. S1 shows a reduction of atrophic fibers upon SSPN overexpression. Online supplemental material is available at http://www.jcb.org/cgi/content/full/jcb.200808027/DC1.

We kindly thank Drs. M. Spencer and S. Lopez for their expertise with whole quadriceps imaging and quantitative PCR analysis.

A.K. Peter was supported by the Molecular, Cellular, and Integrative Physiology predoctoral training fellowship (National Institutes of Health grant T32 GM65823), the Edith Hyde Fellowship, the Ursula Mandel Fellowship, and the Harold and Lillian Kraus American Heart Predoctoral Fellowship. J.L. Marshall was supported by the Genetics Predoctoral Training Fellowship (U.S. Public Health Service National Research Service Award GM07104). R.H. Crosbie was supported by the National Institutes of Health (grant AR48179-01).

Submitted: 6 August 2008
Accepted: 1 October 2008

## References

Barresi, R., and K.P. Campbell. 2006. Dystroglycan: from biosynthesis to pathogenesis of human disease. *J. Cell Sci.* 119:199–207.

Campbell, K.P., and S.D. Kahl. 1989. Association of dystrophin and an integral membrane glycoprotein. *Nature.* 338:259–262.

Crawford, G.E., J.A. Faulkner, R.H. Crosbie, K.P. Campbell, S.C. Froehner, and J.S. Chamberlain. 2000. Assembly of the dystrophin-associated protein complex does not require the dystrophin COOH-terminal domain. *J. Cell Biol.* 150:1399–1410.

Crosbie, R.H., J. Heighway, D.P. Venzke, J.C. Lee, and K.P. Campbell. 1997. Sarcospan: the 25-kDa transmembrane component of the dystrophin-glycoprotein complex. *J. Biol. Chem.* 272:31221–31224.

Crosbie, R.H., H. Yamada, D.P. Venzke, M.P. Lisanti, and K.P. Campbell. 1998. Caveolin-3 is not an integral component of the dystrophin-glycoprotein complex. *FEBS Lett.* 427:279–282.

Crosbie, R.H., C.S. Lebakken, K.H. Holt, D.P. Venzke, V. Straub, J.C. Lee, R.M. Grady, J.S. Chamberlain, J.R. Sanes, and K.P. Campbell. 1999. Membrane targeting and stabilization of sarcospan is mediated by the sarcoglycan subcomplex. *J. Cell Biol.* 145:153–165.

DelloRusso, C., J.M. Scott, D. Hartigan-O'Connor, G. Salvatori, C. Barjot, A.S. Robinson, R.W. Crawford, S.V. Brooks, and J.S. Chamberlain. 2002. Functional correction of adult *mdx* mouse muscle using gutted adenoviral vectors expressing full-length dystrophin. *Proc. Natl. Acad. Sci. USA.* 99:12979–12984.

Durbeej, M., and K.P. Campbell. 2002. Muscular dystrophies involving the dystrophin-glycoprotein complex: an overview of current mouse models. *Curr. Opin. Genet. Dev.* 12:349–361.

Ervasti, J.M., and K.P. Campbell. 1991. Membrane organization of the dystrophin-glycoprotein complex. *Cell.* 66:1121–1131.

Ervasti, J.M., and K.P. Campbell. 1993. A role for the dystrophin-glycoprotein complex as a transmembrane linker between laminin and actin. *J. Cell Biol.* 122:809–823.

Ervasti, J.M., K. Ohlendieck, S.D. Kahl, M.G. Gaver, and K.P. Campbell. 1990. Deficiency of a glycoprotein component of the dystrophin complex in dystrophic muscle. *Nature.* 345:315–319.

Ervasti, J.M., S.D. Kahl, and K.P. Campbell. 1991. Purification of dystrophin from skeletal muscle. *J. Biol. Chem.* 266:9161–9165.

Grady, R.M., H. Zhou, J.M. Cunningham, M.D. Henry, K.P. Campbell, and J.R. Sanes. 2000. Maturation and maintenance of the neuromuscular synapse: genetic evidence for roles of the dystrophin–glycoprotein complex. *Neuron.* 25:279–293.

Gregorevic, P., J.M. Allen, E. Minami, M.J. Blankinship, M. Haraguchi, L. Meuse, E. Finn, M.E. Adams, S.C. Froehner, C.E. Murry, and J.S. Chamberlain. 2006. rAAV6-microdystrophin preserves muscle function and extends lifespan in severely dystrophic mice. *Nat. Med.* 12:787–789.

Hemler, M.E. 2003. Tetraspanin proteins mediate cellular penetration, invasion, and fusion events and define a novel type of membrane microdomain. *Annu. Rev. Cell Dev. Biol.* 19:397–422.

Holt, K.H., and K.P. Campbell. 1998. Assembly of the sarcoglycan complex. Insights for muscular dystrophy. *J. Biol. Chem.* 273:34667–34670.

Jasmin, B.J., H. Alameddine, J.A. Lunde, F. Stetzkowski-Marden, H. Collin, J.M. Tinsley, K.E. Davies, F.M. Tome, D.J. Parry, and J. Cartaud. 1995. Expression of utrophin and its mRNA in denervated *mdx* mouse muscle. *FEBS Lett.* 374:393–398.

Judge, L.M., M. Haraguchiln, and J.S. Chamberlain. 2006. Dissecting the signaling and mechanical functions of the dystrophin-glycoprotein complex. *J. Cell Sci.* 119:1537–1546.

Levy, S., and T. Shoham. 2005. The tetraspanin web modulates immune-signalling complexes. *Nat. Rev. Immunol.* 5:136–148.

Matsumura, K., J.M. Ervasti, K. Ohlendieck, S.D. Kahl, and K.P. Campbell. 1992. Association of dystrophin-related protein with dystrophin-associated proteins in *mdx* mouse muscle. *Nature.* 360:588–591.

Menke, A., and H. Jockusch. 1991. Decreased osmotic stability of dystrophin-less muscle cells from the mdx mouse. *Nature.* 349:69–71.

Michele, D.E., and K.P. Campbell. 2003. Dystrophin-glycoprotein complex: post-translational processing and dystroglycan function. *J. Biol. Chem.* 278:15457–15460.

Miller, G., E.L. Wang, K.L. Nassar, A.K. Peter, and R.H. Crosbie. 2007. Structural and functional analysis of the sarcoglycan-sarcospan subcomplex. *Exp. Cell Res.* 313:639–651.

Odom, G.L., P. Gregorevic, and J.S. Chamberlain. 2007. Viral-mediated gene therapy for the muscular dystrophies: successes, limitations, and recent advances. *Biochim. Biophys. Acta.* 1772:243–262.

Ohlendieck, K., and K.P. Campbell. 1991. Dystrophin-associated proteins are greatly reduced in skeletal muscle from mdx mice. *J. Cell Biol.* 115: 1685–1694.

Peter, A.K., and R.H. Crosbie. 2006. Hypertrophic response of Duchenne and limb-girdle muscular dystrophies is associated with activation of Akt pathway. *Exp. Cell Res.* 312:2580–2591.

Peter, A.K., G. Miller, and R.H. Crosbie. 2007. Disrupted mechanical stability of the dystrophin-glycoprotein complex causes severe muscular dystrophy in sarcospan transgenic mice. *J. Cell Sci.* 120:996–1008.

Petrof, B.J., J.B. Shrager, H.H. Stedman, A.M. Kelly, and H.L. Sweeney. 1993. Dystrophin protects the sarcolemma from stresses developed during muscle contraction. *Proc. Natl. Acad. Sci. USA.* 90:3710–3714.

Spencer, M.J., J.R. Guyon, H. Sorimachi, A. Potts, I. Richard, M. Herasse, J. Chamberlain, I. Dalkilic, L.M. Kunkel, and J.S. Beckmann. 2002. Stable expression of calpain 3 from a muscle transgene in vivo: immature muscle in transgenic mice suggests a role for calpain 3 in muscle maturation. *Proc. Natl. Acad. Sci. USA.* 99:8874–8879.

Straub, V., J.A. Rafael, J.S. Chamberlain, and K.P. Campbell. 1997. Animal models for muscular dystrophy show different patterns of sarcolemmal disruption. *J. Cell Biol.* 139:375–385.

Tinsley, J.M., A.C. Potter, S.R. Phelps, R. Fisher, J.I. Trickett, and K.E. Davies. 1996. Amelioration of the dystrophic phenotype of *mdx* mice using a truncated utrophin transgene. *Nature.* 384:349–353.

Tinsley, J., N. Deconinck, R. Risher, D. Kahn, S. Phelps, J.M. Gillis, and K. Davies. 1998. Expression of full-length utrophin prevents muscular dystrophy in *mdx* mice. *Nat. Med.* 4:1441–1444.

Weller, B., G. Karpati, and S. Carpenter. 1990. Dystrophin-deficient *mdx* muscle fibers are preferentially vulnerable to necrosis induced by experimental lengthening contractions. *J. Neurol. Sci.* 100:9–13.

Yoshida, M., and E. Ozawa. 1990. Glycoprotein complex anchoring dystrophin to sarcolemma. *J. Biochem. (Tokyo).* 108:748–752.